

1 **Introgression in *Brownea* suggests that reticulate evolution**
2 **contributes to Amazonian tree diversity**

3 Rowan J. Schley^{1,2*}, R. Toby Pennington^{3,4}, Oscar Alejandro Pérez-Escobar¹, Andrew J. Helmstetter⁵,
4 Manuel de la Estrella⁶, Isabel Larridon^{1,7}, Izai Alberto Bruno Sabino Kikuchi^{1,8},
5 Timothy Barraclough², Félix Forest¹, and Bente Klitgård¹

6
7 ¹*Royal Botanic Gardens, Kew, Richmond, Surrey, TW9 3AE, UK*

8 ²*Department of Life Sciences, Imperial College London, Silwood Park, Ascot, Berkshire, UK, SL5 7PY*

9 ³*Geography, University of Exeter, Laver Building, North Park Road, Exeter EX4 4QE*

10 ⁴*Royal Botanic Garden Edinburgh, 20a Inverleith Row, Edinburgh EH3 5LR*

11 ⁵*Institut de Recherche pour le Développement (IRD), UMR-DIADE, BP 64501, F-34394 Montpellier cedex 5, France.*

12 ⁶*Departamento de Botánica, Ecología y Fisiología Vegetal, Facultad de Ciencias, Campus de Rabanales, Universidad de Córdoba,*
13 *14071, Córdoba, Spain*

14 ⁷*Systematic and Evolutionary Botany Lab, Department of Biology, Ghent University, K.L. Ledeganckstraat 35, 9000 Gent, Belgium*

15 ⁸*Universiteit Leiden, Hortus botanicus Leiden, PO Box 9500, Leiden, 2300 RA, The Netherlands*

16
17
18 *Corresponding author at: Room E.2.6, Herbarium, Royal Botanic Gardens, Kew, Richmond, Surrey, TW9 3AE, UK

19 E-mail address: r.schley@kew.org (R. J. Schley).

20
21 **Abstract**

22 Hybridization has the potential to generate or homogenize biodiversity and is a particularly common
23 phenomenon in plants, with an estimated 25% of species undergoing inter-specific gene flow.

24 However, hybridization has rarely been demonstrated among tree species in Amazonia, the world's
25 largest rainforest. We show that within *Brownea*, a characteristic tree genus of Amazonia, there is
26 extensive evidence of hybridization. Using both phylogenomic and population genomic approaches
27 we find multiple historical hybridization events within *Brownea*, along with contemporary
28 hybridization among co-occurring species. Finally, we infer homogeneous rates of gene flow among
29 different genomic loci, indicating a lack of selection against hybrids, reflecting their persistence over
30 time. These results demonstrate that gene flow between Amazonian tree species has occurred across
31 temporal scales and may have contributed to the evolution of the most diverse tree flora on Earth.

32

33 Introduction

34 Reproductive isolation is often seen as a prerequisite for speciation and as a defining feature of
35 species^{1,2}. Despite this, hybridization between species is known to occur, and has several different
36 outcomes, from the erosion of evolutionary divergence^{3,4} to the formation of entirely new ‘hybrid
37 species’⁵. Neotropical rainforests harbour the highest levels of plant diversity on Earth⁶, and to date
38 there has been little convincing evidence that hybridization consistently occurs between tree species
39 therein. Indeed, the prevailing view has been that hybridization between tropical tree species is an
40 exceptionally rare event⁷⁻⁹. Although a few observations of reproductive biology support this, such as
41 the intersterility between lineages of *Inga*, a species-rich genus in the legume family¹⁰, evidence for
42 hybridization has been poorly tested empirically in tropical floras. The only potential example of
43 hybridization among neotropical trees which has been documented using DNA sequence data
44 involves two species of *Carapa*¹¹ found in Amazonia, the largest expanse of rainforest in the world
45 which contains at least 6,800 tree species¹².

46 One factor that suggests hybridization might occur more frequently in neotropical rainforest tree
47 species, if their reproductive isolation is not absolute, is the remarkable level of sympatry found for
48 closely related species. In several neotropical lineages, including *Inga*, *Guatteria* and *Swartzia*, many
49 recently diverged species co-occur¹³, often to a remarkable degree. One such example of this is the
50 co-occurrence of 19 *Inga* species in a single hectare of the Ecuadorian Amazon¹⁴. As such, for many
51 rainforest taxa the opportunity for hybridization is constantly present.

52 Hybridization can have a range of evolutionary consequences. In many cases, hybridization simply
53 results in the formation of sterile, maladapted offspring with poor reproductive fitness, allowing
54 genetic isolation between species to be maintained (i.e., reinforcement¹⁵). In other cases, there may be
55 a permanent movement of genetic material from one lineage to another¹⁶, which is known as
56 ‘introgression’. This transfer of genetic material through hybridization may confer a selective
57 advantage to resultant offspring¹⁷, in which case it is referred to as ‘adaptive introgression’. Adaptive

58 introgression is most often observed between closely-related taxa during the invasion of new habitats
59 ^{18, 19}. Furthermore, hybridization can lead to rapid evolutionary radiations. This occurs through the re-
60 assembly of standing genetic variation which has accumulated between diverging lineages, and which
61 has already been subject to selection. This ‘combinatorial’ process is much more rapid than the
62 gradual accumulation of variation through mutation, and the passage of these variants through
63 hybridization often fuels rapid diversification events ²⁰. This has been demonstrated in a wide range of
64 taxa, including sunflowers, African cichlid fish and Darwin’s finches ²¹⁻²³.

65 Introgression can occur at different rates in different regions of the genome ²⁴. Regions under
66 divergent selection may remain distinct due to reduced fitness of hybrid genotypes at such loci,
67 resulting in a low rate of introgression. Conversely, regions under little or no selection tend to
68 introgress more freely, becoming homogenised between species. Moreover, if there is selection for
69 hybrid genotypes (as in adaptive introgression), the rate of introgression for a region may be further
70 increased relative to the rest of the genome ²⁵. Such a process has been demonstrated in temperate-
71 zone tree species, where divergence between hybridizing lineages is maintained through
72 environmentally-driven selection ^{26, 27}. This explains why species that hybridize can remain as
73 biologically distinct (and taxonomically identifiable) groups despite undergoing genetic exchange
74 with other species ^{28, 29}.

75 *Brownea*, a member of the pea and bean family (Fabaceae/Leguminosae), is a characteristic tree
76 genus of lowland neotropical rainforests, and contains around 27 species distributed across northern
77 South America. Previous work indicates that there is a broad degree of phylogenetic incongruence
78 evident in this genus ³⁰ which might indicate hybridization, although this could also result from
79 incomplete lineage sorting (the differential inheritance of genetic variation from a common ancestral
80 species in different descendent lineages). However, there are numerous *Brownea* hybrids in
81 cultivation (e.g. *B. x crawfordii* ³¹ and *B. hybrida* ³²), as well as several instances of putative
82 hybridization among *Brownea* lineages in the wild. The most notable of these instances is that
83 proposed between the range-restricted *Brownea jaramilloi* ³³ and the wide-ranging *B. grandiceps*,
84 which co-occur in the Ecuadorian Amazon (Fig. 1). There are multiple morphological distinctions

85 between these two species, including differences in inflorescence colour and structure, growth habit,
86 tree height and leaf morphology³³. Although they co-occur, these species favour different habitats: *B.*
87 *jaramilloi* grows on ridge tops and hillsides, whereas *B. grandiceps* shows a slight preference for
88 swamps and valleys but is more evenly distributed^{33,34}. Despite this, hybridization appears to occur,
89 as evidenced by the existence of a putative hybrid between these two species known as *B. "rosada"*
90 (Fig. 1). *Brownea "rosada"* displays an intermediate morphology between its two parental species,
91 producing pink flowers. The hypothesis of a *B. jaramilloi* x *B. grandiceps* hybrid has not yet been
92 tested, however, using molecular data.



95 As a member of the legume family, which dominates Amazonian forests³⁵, and with its apparent
96 propensity for hybridization, *Brownea* is an excellent system with which to study the phylogenetic
97 patterns and genomic architecture of introgression in neotropical rainforest trees. Systematically
98 documenting hybridization at a range of time scales and taxonomic levels within this group could
99 reveal how admixture has contributed to the assembly of one of the world's richest floras.

100 Accordingly, this investigation aims to answer the following questions:

101

- 102 1. Is there evidence of hybridization at a deep phylogenetic level in this lineage of neotropical
103 rainforest tree?

104 2. Is there evidence of more recent gene flow, and if so, does this occur evenly across most of
105 the genome?

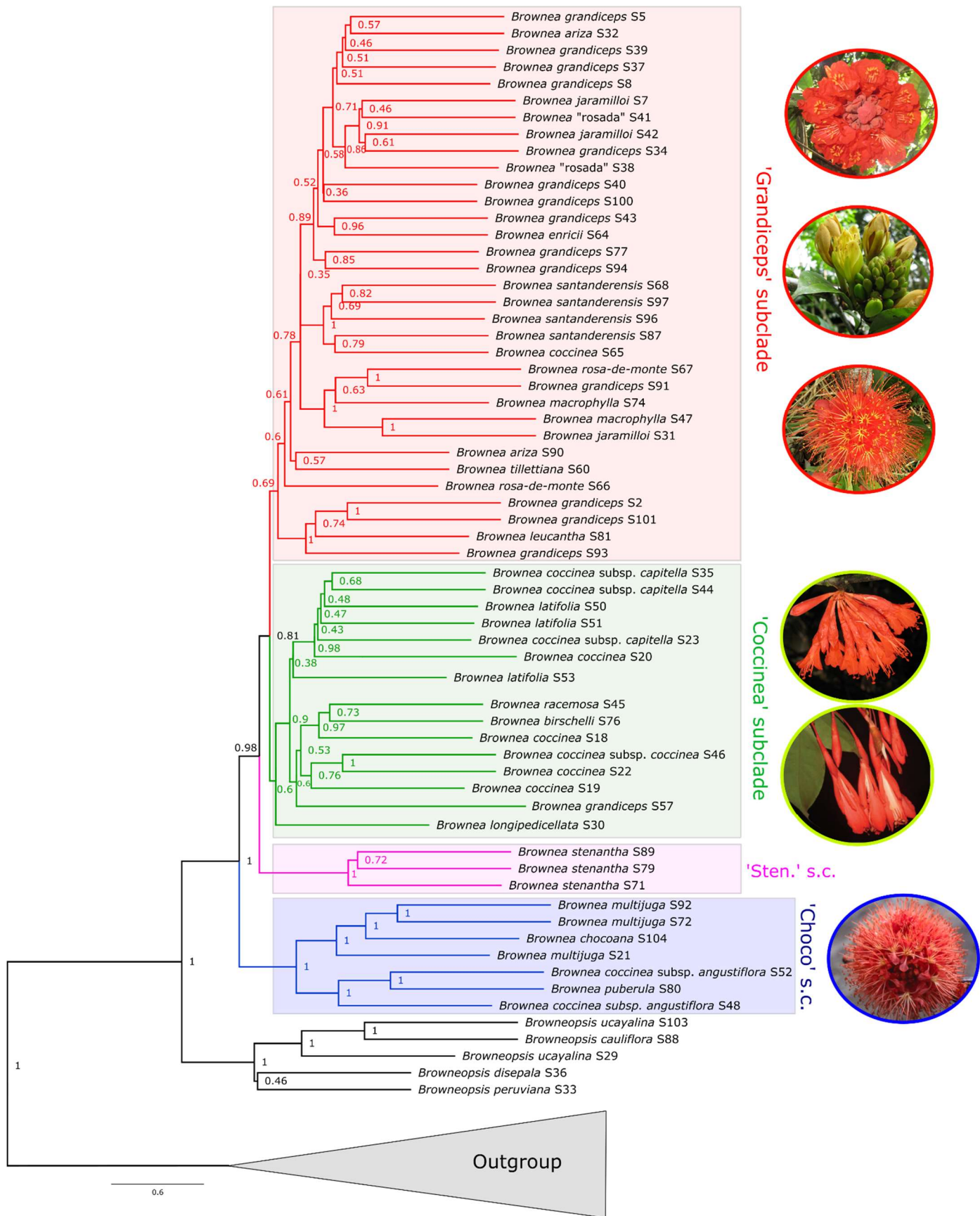
106

107 Results

108 Phylogenetic analysis

109 Using DNA sequence data from 226 nuclear gene regions, we produced a ‘species’ tree using
110 *ASTRAL*³⁶ (Fig. 2) based on gene trees inferred with the program *RAxML*³⁷. This resulted in well-
111 supported relationships between major subclades (>0.9 local posterior probability (PP)), with lower
112 support for inter-specific relationships. *ASTRAL* inferred that 50.2% of gene tree quartets were
113 congruent with the ‘species’ tree. There was a high degree of discordance among gene tree topologies
114 at many nodes, with multiple alternative bipartitions reconstructed at most nodes. This is evident from
115 the presence of many more conflicting gene trees (numbers below branches) than congruent gene
116 trees (numbers above branches) in Supplementary Fig. 1.

117



118

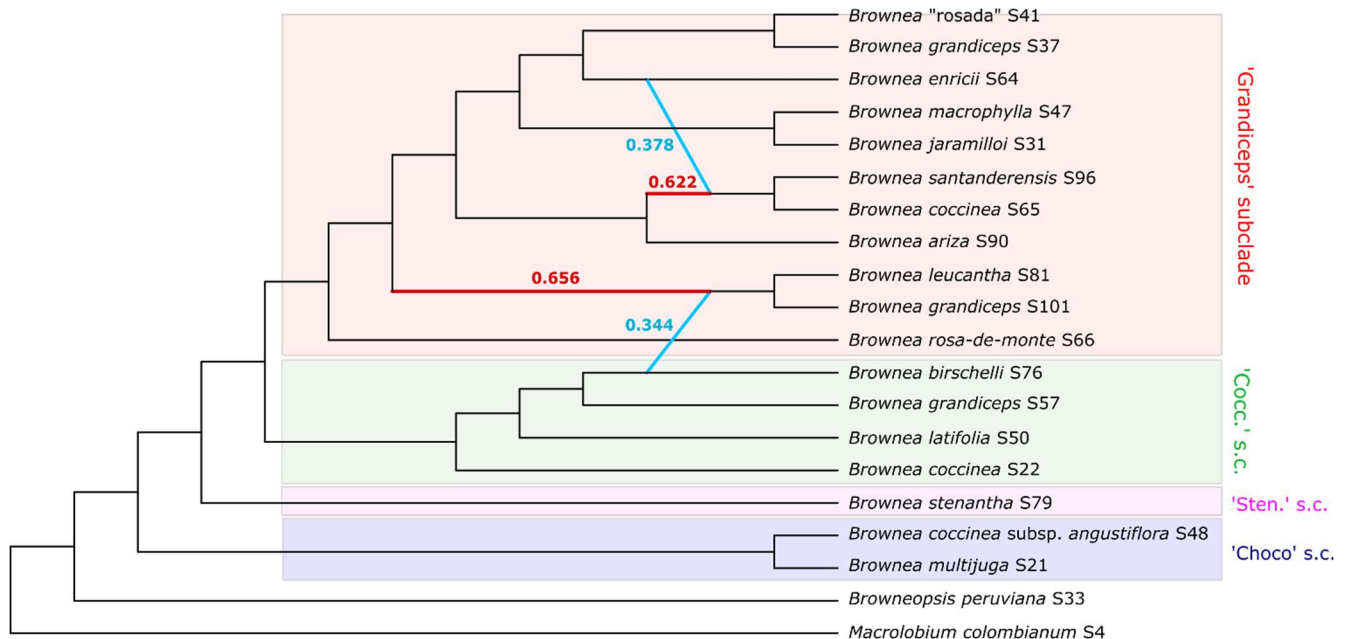
119

120

121 Ancient introgression in *Brownea* species

122 Phylogenetic networks were estimated using concordance factors (CF) generated from *RAxML* gene
123 trees to ascertain whether the historical pattern of diversification in *Brownea* was tree-like or
124 reticulate. Networks with different numbers of hybridization events (h) were compared using -log
125 pseudolikelihoods. The best-fitting network model was $h = 2$, as indicated by the -log
126 pseudolikelihood values displayed in Supplementary Fig. 2, suggesting that there were two
127 hybridization events within the *Brownea* taxa sampled for this study. Negative log pseudolikelihoods
128 increased steadily between $h = 0$ and $h = 2$, after which the increasing number of hybridization events
129 only make minimal improvements to -log pseudolikelihood.

130



131

132

133 The inferred phylogenetic network (Fig. 3) showed a broadly similar topology to the species tree in
134 Fig. 2, with the addition of two hybridization events. The first hybridization event occurred between
135 the lineage leading to the Venezuelan accessions of *B. grandiceps*/*B. leucantha* and *B. birschelli*,

136 suggesting that the lineage leading to *B. birschelli* has in the past contributed around 34% of the
137 genetic material present in the common ancestor of the Venezuelan *B. grandiceps* and *B. leucantha*.
138 The second inferred occurrence of hybrid ancestry occurs between the ancestors of the subclade
139 containing the Colombian accessions of *B. coccinea*/*B. santanderensis* and the lineage leading to *B.*
140 *enricii*, which contributed around 37% of the genetic material belonging to the ancestor of the
141 aforementioned subclade.

142 TICR (Tree Incongruence Checking in R) analysis indicated that a network-like model best described
143 the patterns of incongruence in the single-accession-per-species gene trees inferred during this study.
144 This method suggested an excess of outlier quartets ($P = 1.240 \times 10^{-19}$, $X^2 = 91.149$), which differed
145 significantly from the CF values expected under a model containing only incomplete lineage sorting.
146 As such, a tree-like model was able to be rejected as an explanation for the observed relationships
147 between taxa in *Brownea*, suggesting that hybridization occurred over the course of its evolutionary
148 history.

149

150 Introgression dynamics across loci

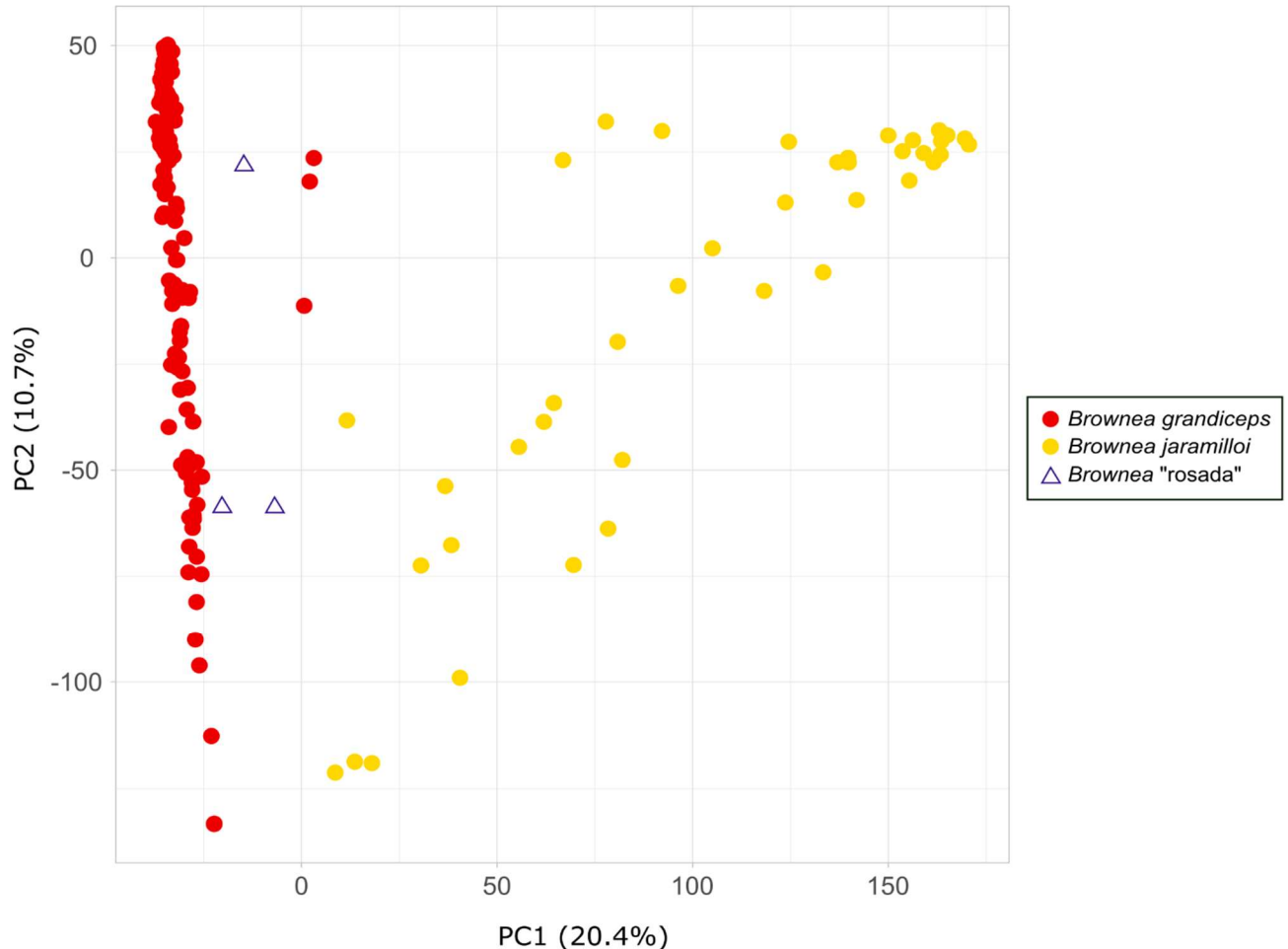
151 Having examined the degree of historical reticulation among *Brownea* lineages, population genomic
152 data were generated with ddRAD sequencing and used to investigate recent introgression at a finer
153 taxonomic scale. More specifically, the degree of shared genetic variation was visualised for co-
154 occurring individuals of *B. grandiceps* and *B. jaramilloi*, which putatively hybridize in the wild.
155 Following this, in order to make inferences about the potential evolutionary significance of recent
156 introgression, the rates at which different loci introgress relative to the rest of the genome were
157 estimated for these taxa using genomic clines.

158 In total, ddRAD sequencing resulted in 640,898,950 reads between 350-550bp in length for 171
159 individuals. Among these reads, 28,503,796 (4.45%) were discarded due to poor recovery. There was
160 a mean of 3,747,947 reads per individual, with an average coverage depth across all samples of 27.5x.

161 Relatively high levels of shared genetic variation were observed among taxa, along with low levels of
162 genetic differentiation and only marginal differences in the amount of genetic variation, as shown by
163 the population genetic statistics calculated by the Stacks pipeline for the two *Brownea* species
164 (including *B. “rosada”*, which is grouped with *B. grandiceps*) (Supplementary Table 3). The F_{st}
165 calculated between *B. grandiceps*/*B. “rosada”* and *B. jaramilloi* was 0.111, representing a low degree
166 of fixation, and so a high amount of shared variation.

167 Patterns of shared genetic variation were visualised using principal component analysis (PCA) and a
168 genetic distance network inferred with the program *SPLITSTREE*³⁸. These analyses indicated a
169 distinct signature of admixture between *B. grandiceps* and *B. jaramilloi*. The PCA of SNP variation
170 inferred using the R package *ggplot2* (Fig. 4) indicated that the first principal component (PC1)
171 explained the largest proportion of the genetic variation among all the principal components (20.4%).
172 Individuals of *B. grandiceps* are tightly clustered along PC1, where the individuals of *B. jaramilloi*
173 show much more variability, with many individuals forming an intergradation between the two main
174 species clusters. Additionally, the *B. “rosada”* accessions appear to have clustered more closely to *B.*
175 *grandiceps* than to *B. jaramilloi* along PC1. PC2, which explained 10.7% of the variation in the SNP
176 data, shows a similar degree of variability in both *B. grandiceps* and *B. jaramilloi*, with two
177 accessions of *B. “rosada”* shown to cluster in between both species. This pattern is reflected by the
178 implicit network built using *SPLITSTREE* (Supplementary Fig. 3). *SPLITSTREE* recovered a
179 clustering of individuals into two main groups, largely representing *B. grandiceps* and *B. jaramilloi*,
180 with four putative hybrid individuals displaying an intermediate relationship between the two species
181 clusters.

182



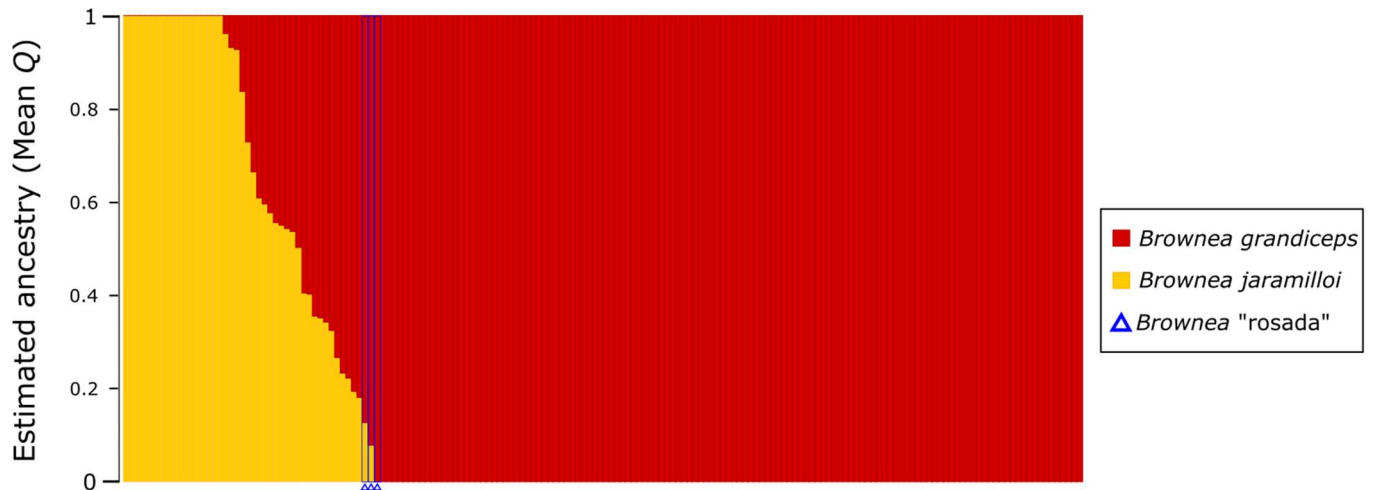
183

184

185 A *fastSTRUCTURE* analysis³⁹ was performed to further examine the degree of shared genetic
186 variation, as well as providing information on the population genetic structure of the two species. This
187 analysis indicated that there was a large amount of shared ancestry between the genotyped individuals
188 (Fig. 5), with evidence of extensive backcrossing due to the widely differing proportions of ancestry
189 in different individuals. Marginal likelihood comparison indicated that the best value of K (i.e., the
190 number of populations) was two, which was the value that resulted in the largest increase in marginal
191 likelihood ($\Delta_{\text{marginal likelihood}} = 0.085$, Supplementary Fig. 4A)). Since the ‘best’ value of K is an
192 estimate, *fastSTRUCTURE* plots generated with other K values are shown in Supplementary Fig. 4B.
193 In Fig. 5, it appears that most individuals identified as *B. jaramilloi* have, at least in part, some *B.*
194 *grandiceps* ancestry. In addition, the individuals identified as *B. "rosada"* appear to have inherited
195 most of their ancestry from *B. grandiceps*, with only a minimal contribution from *B. jaramilloi*. The

196 same pattern was recovered from a *fastSTRUCTURE* run incorporating 40 random individuals from
197 each species, performed to account for any bias which may have been incurred by differences in
198 sample size (Supplementary Fig. 4C).

199



200

201

202 A *NEWHYBRIDS* analysis ⁴⁰ (<https://github.com/eriqande/newhybrids>) was used to categorize 169 of
203 171 genotyped individuals into different hybrid classes (pure, F1, F2, and backcrosses). This was
204 performed on three subsets of 500 loci due to the computational limitations of the program.

205 *NEWHYBRIDS* revealed that most hybrid individuals were the result of continued hybridization, with
206 pure *B. grandiceps* making up 73.9% of the genotyped population, and pure *B. jaramilloi* making up
207 21.9%. There were no F1 (first generation) hybrids identified by the subset of loci analysed, and all
208 hybrid individuals were either F2 hybrids (0.592%) or had a broad distribution of probabilities across
209 hybrid classes (3.55%). In the latter, the probability of any one hybrid class did not exceed 90%,
210 which was the threshold used to categorize individuals as belonging to a certain class.

211 Bayesian estimation of genomic clines (*bgc*) was utilised to determine whether any loci showed
212 outlying rates of admixture relative to the genome-wide average among all genotyped individuals.
213 This method estimates two parameters for each locus: α (the 'direction' of introgression) and β (the
214 'rate' of introgression), which were used to infer the impact of selection on introgressing loci. *bgc*

215 recovered a signal of asymmetric introgression but did not detect any differential rates of
216 introgression between loci. Of the 19,130 loci under study, *bgc* recovered 251 loci (1.3%) with mostly
217 *B. jaramilloi* alleles among all individuals (i.e. with positive α estimates) and 1089 loci (5.69%) with
218 mostly *B. grandiceps* alleles among all individuals (i.e., with negative α estimates). However, no loci
219 displayed extreme rates of introgression relative to the average rate across the genome (i.e., there were
220 no statistically outlying β parameter estimates). The MCMC runs from which these results were
221 drawn showed adequate mixing (Supplementary Fig. 5A-C).

222

223 Discussion

224 Our study represents the clearest documented case of reticulated evolution among Amazonian trees,
225 which was previously seen as an extremely rare phenomenon. We demonstrate that within *Brownea*, a
226 characteristic Amazonian tree genus, reticulated evolution has occurred over the course of its
227 evolutionary history, with evidence of introgression deep in the history of the genus and more
228 recently, between the closely related *B. grandiceps* and *B. jaramilloi*.

229 Phylogenetic network analysis suggested that introgression has taken place between *Brownea* lineages
230 in the past, with two separate hybridization events inferred and displayed in Fig. 3. The concordance
231 factors obtained from gene trees were not adequately explained by a tree-like model (i.e., one
232 accounting only for incomplete sorting of ancestral variation), suggesting that a network-like model
233 (i.e., one including introgression) best describes the diversification patterns within *Brownea* ($P=$
234 1.240×10^{-19} , $X^2 = 91.149$). Hybridization mainly occurs between individuals which are
235 geographically overlapping, or have been so at some point in the past⁴¹. Our findings are thus further
236 corroborated by the fact that both historical introgression events were between taxa that co-occur
237 (e.g., *B. grandiceps*, *B. leucantha* and *B. birschelli* on the Northern coast of Venezuela, and *B.*
238 *coccinea*, *B. santanderensis* and *B. enricii* within the Colombian cordilleras). This is also in
239 agreement with previous work³⁰, which indicated that the ‘stem’ lineages within *Brownea* shared a
240 broad distribution across northern South America, which may have further facilitated earlier

241 hybridization. Our study also recovered a low degree of support for inter-specific relationships (Fig.
242 2) and a high degree of incongruence among gene trees (Supplementary Fig. 1). These results can be
243 partially explained by introgression, rather than being caused purely by the stochasticity of lineage
244 sorting in large populations, which is suggested to be a common phenomenon in many rainforest trees
245 with large population sizes⁴². It seems that amongst closely-related species of *Brownea* it is likely that
246 divergence has not progressed to the point of complete reproductive isolation, as has been shown in
247 temperate *Quercus* species⁴³. Moreover, the low quartet scores and minimal gene-tree concordance
248 found at the species level in this study mirror those observed in *Lachemilla*, a montane neotropical
249 plant genus, in which gene tree discordance was shown to be explained by both historical and recent
250 hybridization⁴⁴.

251 Since the inferred events of ancient introgression both involved the common ancestors of two sets of
252 present-day species, they are likely to have occurred several million years in the past, before the
253 divergence of the descendent species. The inferred introgression events are likely to have occurred
254 since the Miocene period (~23Ma), as date estimates from previous work suggest that *Brownea*
255 originated around this time³⁰. Accordingly, it is unlikely that the inferred hybridization events are due
256 to ‘accidental’ hybridization between co-occurring species, merely producing maladapted F1 hybrids
257 which will eventually be outcompeted, fortifying the boundaries between species (a process known as
258 ‘reinforcement’¹⁵). Rather, our results suggest a persistence of introgression over evolutionary time
259 within *Brownea*.

260 This investigation also uncovered a substantial signal of recent introgression between *B. grandiceps*
261 and *B. jaramilloi* in the Yasuní National Park 50ha plot located in the Ecuadorian Amazon, with
262 evidence of multi-generational ‘backcrossing’, further suggesting that hybridization does not always
263 result in reinforcement. All hybrid individuals exhibited some degree of backcrossing in the
264 *NEWHYBRIDS* analysis, which implies that hybrids persist over time. The low F_{st} estimate for the *B.*
265 *grandiceps*/*B.* “rosada” and *B. jaramilloi* populations (0.11), in addition to the principal component
266 analysis (Fig. 4), the *fastSTRUCTURE* analysis (Fig. 5) and the *SPLITSTREE* plot (Supplementary
267 Fig. 3) indicated a high degree of shared variation between these lineages. All these approaches show

268 that individuals cluster into two main groups, largely representing *B. grandiceps* and *B. jaramilloi*, as
269 well as a set of individuals forming an intergradation between the two main clusters. The individuals
270 which form a part of this intergradation were mostly identified as *B. jaramilloi*, although hybrid
271 individuals are also observed in the *B. grandiceps* cluster. The higher number of variant sites and the
272 higher nucleotide diversity (π) recovered for *B. jaramilloi* (Supplementary Table 3) could also reflect
273 the hybrid ancestry of many individuals identified as this species. A similar introgression-driven
274 increase in nucleotide diversity has been shown in closely-related species of *Mimulus* which undergo
275 asymmetric introgression⁴⁵.

276 The *bgc* analysis indicated that most introgression was asymmetric, with more loci containing mostly
277 *B. grandiceps* alleles (5.96% of all loci) than loci containing mostly *B. jaramilloi* alleles (1.3% of all
278 loci). Importantly, this *bgc* analysis also indicated that gene flow occurs largely at the same rate
279 across loci, since there were no outlying estimates of the β parameter. The excess of *B. grandiceps*
280 ancestry mirrors the asymmetry of introgression suggested by Fig. 5 and is likely driven by the
281 uneven population sizes of the two species. *Brownea jaramilloi* has only ever been observed in a
282 small part of the western Amazon³³ and is much less populous than *B. grandiceps*, which occurs
283 across northern South America. More specifically, the disproportionate donation of alleles from *B.*
284 *grandiceps* may be due to ‘pollen swamping’, whereby pollen transfer from another, more populous
285 species is more likely than pollen transfer from less numerous conspecifics⁴⁶. Pollen swamping can
286 serve as a mechanism of invasion (e.g., in *Quercus*⁴⁷), and the associated asymmetric introgression
287 may lead to the extinction of the rarer species, especially when hybrids are inviable or sterile⁴⁸.
288 However, due to the ongoing introgression evident between *B. grandiceps* and *B. jaramilloi* it appears
289 that hybrids are not always sterile, or at least that ‘foreign’ alleles are not always subject to strong
290 purifying selection. The best evidence of this is the absence of loci with extreme values of the β
291 parameter recovered by our *bgc* analysis. Extreme deviations in β are mainly expected in the presence
292 of gene flow when selection against hybrids is strong, resulting in underdominance and a paucity of
293 heterozygous sites²⁵.

294 Further to this, the observed asymmetry in introgression could be caused by selection favouring
295 hybrid genotypes. The transfer of genomic regions which confer a selective advantage from a donor to
296 a recipient species (i.e. adaptive introgression) can result in a disproportionate amount of one species'
297 genome being present in hybrid individuals⁴⁹. This occurs when viable hybrids only tend to backcross
298 with one of the parental species, thereby introducing the other species' genetic material into the first
299 in an asymmetrical fashion. Selection has been suggested as a driver for asymmetric introgression in
300 multiple plant genera, including *Helianthus*⁵⁰ and *Iris*⁵¹. Accordingly, it is possible that selectively
301 advantageous alleles are passing between species (e.g., between *B. jaramilloi* and *B. grandiceps*)
302 through backcrossing events over many generations as observed by the *fastSTRUCTURE* and
303 *NEWHYBRIDS* analyses in this study⁵². This may facilitate adaptation to new niches due to the
304 widening of the pool of variation upon which selection can act¹⁸. However, it is difficult to ascertain
305 whether adaptive introgression has occurred without measuring the impact of introgression on
306 variation in the phenotype and its fitness effects¹⁹.

307 Studies such as ours that document hybridization between tree species within Amazonia, and within
308 tropical rainforests in general, are rare. Indeed, it was previously suggested that interspecific hybrids
309 between rainforest tree species are poor competitors, and that fertile hybrid populations are nearly
310 non-existent⁸. While there is some evidence of introgression in tropical trees¹¹, most available studies
311 substantiating this are based on trees from other tropical regions or habitats (e.g., *Shorea* in Asia^{53,54},
312 or *Rhizophora* in Indo-Pacific mangroves⁵⁵). Many of these other instances appear to occur only in
313 degraded habitats, or involve infertile first-generation hybrids with minimal backcrossing, which
314 contrasts with the findings of our study. Within *Brownea* we found evidence of introgression across
315 taxonomic, spatial and temporal scales, with evidence of backcrossing and a lack of selection against
316 hybrid genotypes. It is possible that a lack of selection against hybrids allows the passage of variation
317 between *Brownea* species, which may persist over evolutionary time and could help explain why we
318 found evidence of introgression both at macroevolutionary and microevolutionary scales. While it is
319 difficult to determine whether hybridization between Amazonian tree lineages is a more common
320 occurrence than previously thought, or whether it is a tendency unique to certain rainforest genera

321 such as *Brownea*, it may be prudent to review how relationships among tropical tree lineages are
322 inferred. Accordingly, in order to understand the evolutionary relationships within such groups using
323 phylogenetic networks may provide additional insight into whether reticulate evolution has
324 contributed to diversification within Amazonian rainforest, which is among the most species-rich
325 environments on Earth ^{41, 56}.

326

327 Methods

328 Phylogenetic analysis

329 Sequences from 226 nuclear genes were used to elucidate the evolutionary relationships between
330 *Brownea* species using a phylogenomic approach. DNA sequence data were generated from leaf
331 material collected from herbarium specimens and silica-gel dried accessions using targeted bait
332 capture. Targeted bait capture uses RNA probes to enable the sequencing of fragmented DNA, such as
333 that collected from historical natural history collections. Details of library preparation, hybridization
334 and sequencing are detailed in Supplementary Methods 1. Twenty-three of twenty-seven lineages
335 were sampled within the genus *Brownea*, including the three subspecies of *B. coccinea* and one
336 putative hybrid lineage (*Brownea* “rosada”, a putative hybrid of *B. grandiceps* and *B. jaramilloi*). In
337 total, 59 accessions were sampled within *Brownea*, as well as an additional 13 outgroup taxa from the
338 genera *Macrolobium*, *Heterostemon*, *Paloue* and *Browneopsis*, which form part of the ‘*Brownea*
339 clade’ (Leguminosae, subfamily Detarioideae ⁵⁷). The list of accessions and their associated
340 information can be found in Supplementary Table 1.

341 DNA sequencing reads were quality-checked with the program *FASTQC* v0.11.3 ⁵⁸, and were
342 subsequently trimmed using *Trimmomatic* v.0.3.6 ⁵⁹. This was done to remove adapter sequences and
343 to quality-filter reads, by removing reads that were too short or of poor quality, as assessed by their
344 phred-33 score. Following quality-filtering, loci were assembled using *SPAdes* v3.11.1 ¹⁶ by the
345 HybPiper pipeline v1.2 ⁶⁰, and potentially paralogous loci were removed using the Python ⁶¹ script
346 ‘*paralog_investigator.py*’, distributed with the HybPiper pipeline. All sequences were aligned by gene

347 region using *MAFFT* v7.215⁶². In order to infer gene trees for phylogenetic network analysis, the 226
348 gene regions were further refined to include only 20 taxa, representing a single accession per lineage
349 in *Brownea*, using *Macrolobium colombianum* as the outgroup taxon. Where applicable, samples were
350 chosen by comparing the sequence recovery of conspecific accessions and choosing the individual
351 with the best gene recovery. This resulted in 220 single-accession-per-lineage gene alignments.
352 Further details of quality filtering, read assembly and alignment of DNA sequencing reads are given
353 in Supplementary Methods 1.

354 Gene trees were generated for each of the 226 gene alignments using *RAxML* v.8.0.26³⁷ with 1,000
355 rapid bootstrap replicates and the GTRCAT model of nucleotide substitution, which is a parameter-
356 rich model and hence is most suitable for large datasets. *Macrolobium colombianum* was used to root
357 both the full and single-accession dataset analyses since it was the *Macrolobium* accession that was
358 present in the most gene alignments. The gene trees from both datasets were used to generate species
359 trees under the multi-species coalescent model in *ASTRAL* v.5.6.1³⁶. The heuristic version of *ASTRAL*
360 was used because gene trees were estimated for >30 taxa, and the default parameters for the program
361 were used for species tree inference. Monophyly was not enforced for individuals belonging to the
362 same species (the '-a' option in *ASTRAL*). Finally, discordance between gene trees was calculated and
363 visualised for the full dataset using the Java program *PhyParts* v0.0.1⁶³
364 (<https://bitbucket.org/blackrim/phyparts>). The pattern of incongruence between gene trees for each
365 node was then mapped onto the *ASTRAL* species tree using the Python script *PhyPartsPieCharts* v1.0
366 (<https://github.com/mossmatters/MJPythonNotebooks>).

367

368 *Inferring ancient introgression*

369 Phylogenetic networks were inferred for 220 gene trees from the single-accession-per-lineage dataset
370 to understand whether introgression occurred over the course of the evolutionary history of *Brownea*.
371 Networks were inferred with the program *SNaQ!*, implemented in the *Julia* v0.6.4⁶⁴ package
372 *PhyloNetworks* v0.11.0⁵⁶. Networks were estimated using gene trees from the single-accession-per-

373 lineage dataset as per the assumptions of the program, which requires that each tip of the phylogenetic
374 trees represent a single lineage. This dataset contained 20 taxa from the genera *Brownea*, *Browneopsis*
375 and *Macrolobium*. The network with the number of hybridization events (h) best describing the data
376 was chosen using negative log pseudolikelihood comparison. Finally, the topologies of the gene trees
377 were compared with those of the best-fit phylogenetic network and those expected under a coalescent
378 model (i.e., a ‘tree-like’ model which accounts for incomplete lineage sorting but not hybridization).
379 The fit of the observed gene tree topologies to either the ‘network-like’ or the ‘tree-like’ model was
380 assessed using the Tree Incongruence Checking in R (TICR) test ⁶⁵, implemented in the R v3.4.4 ⁶⁶
381 package *PHYLOLM* ⁶⁷. Proportions of genes contributed between lineages by hybridization events
382 were taken from the ‘Gamma value’ output of *PhyloNetworks*. Further details of phylogenetic
383 network analysis are contained in Supplementary Methods 1.

384

385 Population-level introgression

386 The architecture and rates of introgression across the genome were examined using two ecologically
387 divergent *Brownea* species which co-occur in the Ecuadorian Amazon. In order to do this we used
388 ddRADseq ⁶⁸, a reduced-representation genotyping approach which uses restriction enzymes to
389 fragment genomic DNA to generate many thousands of sequence markers *de-novo* for SNP discovery.
390 One-hundred and seventy-one specimens in total were genotyped using dried leaf material. Sampling
391 consisted of 128 individuals of *Brownea grandiceps*, 40 individuals of *B. jaramilloi* and three
392 individuals of *B. “rosada”* (the putative hybrid of *B. grandiceps* and *B. jaramilloi*), representing the
393 relative abundance of each species in the forest plot from which they were sampled. Leaf material was
394 collected from *Brownea* trees in the Yasuni National Park 50ha forest plot in Napo, Ecuador, and
395 dried in a herbarium press. The sample list is shown in Supplementary Table 2. Sampling, library
396 preparation and sequencing protocols are explained further in Supplementary Methods 2.

397 DNA sequencing reads from the ddRADseq genotyping were processed *de novo* (i.e., without the use
398 of a reference genome) using the Stacks pipeline v2.1 ⁶⁹. Reads were quality filtered using Stacks by

399 removing reads which were of poor quality (i.e., had a phred score <10), following which ‘stacks’ of
400 reads were created, and SNPs were identified among all *de novo* ‘loci’ and across individuals. This
401 was done using a minimum coverage depth (the ‘-m’ flag in Stacks) of three and a within-individual
402 mismatch distance (-M) of seven nucleotides. Individuals with sequencing coverage under 7.5x were
403 removed. Loci found in fewer than 40% of individuals and sites with a minor allele frequency
404 threshold of 5% were filtered out using the ‘populations’ module of Stacks.

405 This resulted in a dataset containing 22,046 loci with 120,085 SNPs for 171 individuals. A dataset
406 containing only one SNP per locus was also extracted using the Stacks *populations* module for use in
407 analyses which assumed no linkage disequilibrium. This subsetting resulted in a dataset containing
408 19,130 loci with 19,130 SNPs for 171 individuals. Details of read assembly and filtering are shown in
409 Supplementary Methods 2.

410 In order to understand the patterns of introgression at the population level, the full ddRAD dataset was
411 used to visualise the degree of shared variation between *B. grandiceps* and *B. jaramilloi*. This was
412 performed using principal component analysis implemented in R v3.4.4, followed by plotting with
413 *ggplot2*⁷⁰, and by producing a neighbour net plot in *SPLITSTREE* v4.14.6³⁸. Furthermore, the single-
414 SNP-per-locus dataset containing 19,130 RAD loci was used to infer population structure with the
415 program *fastSTRUCTURE* v1.0³⁹. The number of populations (*K*) was chosen using the value which
416 provided the largest improvement in marginal likelihood. Finally, *NEWHYBRIDS* v1.1⁴⁰

417 (<https://github.com/eriqande/newhybrids>) was used to categorise individuals into different hybrid
418 classes, using three runs of 500 randomly subsetting ddRAD loci. Runs were performed with 50,000
419 MCMC sweeps following 50,000 burn-in sweeps under the default parameters of the program.

420 The relative ‘rate’ and ‘direction’ of introgression for each locus between the two *Brownea* species
421 was estimated using Bayesian estimation of genomic clines (*bgc*) v1.03⁷¹. For each locus, *bgc*
422 compares the probability of ancestry at the locus relative to an individual’s genome wide ancestry,
423 thereby allowing it to estimate two parameters for each locus. These parameters are α , which roughly
424 equates to the ‘direction’ of introgression, and β , which may be summarised as the ‘rate’ of
425 introgression for a locus^{25, 71}. In order to estimate these parameters from the single-SNP dataset

426 consisting of 19,130 RAD loci, 50,000 MCMC generations with a 50% burn-in were used in *bgc*.
427 Admixture proportions (i.e., mean Q values) generated by *fastSTRUCTURE* were used to assign each
428 individual to three populations (*Brownea grandiceps*, *B. jaramilloi* and admixed). Convergence was
429 checked for the MCMC output from *bgc* in Tracer v1.6⁷² and with the R package *coda*⁷³ using
430 Geweke's diagnostic⁷⁴. Loci with significant 'excess ancestry' were identified by ascertaining
431 whether the 99% posterior probability estimates of the α and β parameters included zero (i.e., by
432 identifying positive or negative non-zero estimates of the parameters). In addition, loci which were
433 extreme 'introgression outliers' were identified for both parameters by identifying loci whose median
434 estimates were not included in the 99% posterior probability credible intervals⁷¹. Further details of
435 visualising shared variation, hybrid category assignment and *bgc* analysis are shown in
436 Supplementary Methods 2.

437

438 Data Availability

439 The datasets that support the findings of this study are available from online repositories. All raw
440 reads generated with the targeted bait capture and ddRADseq methods are available on the NCBI
441 Sequence Read Archive with the accession numbers SAMN13439069- SAMN13439140 and
442 SAMN13441804- SAMN13441974, respectively, under the Bioproject number PRJNA592723. All
443 full phylogenomic sequence alignments, single-accession-per-species alignments and tree files, *bgc*
444 input files, Stacks output files and the Detarioideae bait kit sequence file are found on Dryad
445 (<https://doi.org/10.5061/dryad.k3j9kd53w>). The full phylogenomic sequence alignments underlie the
446 phylogeny in Fig. 2, while the single-accession-per-species alignments and tree files underlie Fig. 3.
447 The variant call format (VCF) and Structure files provided on Dryad underlie Fig. 4 and Fig. 5. Data
448 are under embargo until publication, and any further data required are available from the
449 corresponding author upon request. A reporting summary for this article is available as a
450 Supplementary Information file.

451

452

453

References

- 454 1. Mayr, E. in *Systematics and the Origin of Species* (Columbia University Press, New York, New
455 York, USA., 1942).
- 456 2. Barraclough, T. G. in *The Evolutionary Biology of Species* (Oxford University Press, Oxford,
457 2019).
- 458 3. Kearns, A. M. *et al.* Genomic evidence of speciation reversal in ravens. *Nat. Comm.* **9**, 906 (2018).
- 459 4. Vonlanthen, P. *et al.* Eutrophication causes speciation reversal in whitefish adaptive radiations.
460 *Nature* **482**, 357-362 (2012).
- 461 5. Mallet, J. Hybrid speciation. *Nature* **446**, 279-283 (2007).
- 462 6. Antonelli, A. & Sanmartín, I. Why are there so many plant species in the Neotropics? *Taxon* **60**,
463 403-414 (2011).
- 464 7. Ehrendorfer, F. Evolutionary patterns and strategies in seed plants. *Taxon* **19**, 185-195 (1970).
- 465 8. Ashton, P. S. Speciation among tropical forest trees: some deductions in the light of recent
466 evidence. *Biol. J. Linn. Soc.* **1**, 155-196 (1969).
- 467 9. Gentry, A. H. Neotropical floristic diversity: phytogeographical connections between Central and
468 South America, Pleistocene climatic fluctuations, or an accident of the Andean orogeny? *Ann. Mo.*
469 *Bot. Gard.* **69**, 557-593 (1982).
- 470 10. Koptur, S. Outcrossing and pollinator limitation of fruit set: breeding systems of neotropical Inga
471 trees (Fabaceae: Mimosoideae). *Evolution* **38**, 1130-1143 (1984).
- 472 11. Scotti-Saintagne, C. *et al.* Phylogeography of a species complex of lowland Neotropical rain
473 forest trees (Carapa, Meliaceae). *J. Biogeogr.* **40**, 676-692 (2013).
- 474 12. Cardoso, D. *et al.* Amazon plant diversity revealed by a taxonomically verified species list. *Proc.*
475 *Natl. Acad. Sci. U. S. A.* **114**, 10695-10700 (2017).
- 476 13. Dexter, K. G. *et al.* Dispersal assembly of rain forest tree communities across the Amazon basin.
477 *Proc. Natl. Acad. Sci. U. S. A.* **114**, 2645-2650 (2017).
- 478 14. Valencia, R., Balslev, H. & Miño, G. P. Y. High tree alpha-diversity in Amazonian Ecuador.
479 *Biodiversity & Conservation* **3**, 21-28 (1994).
- 480 15. Hopkins, R. Reinforcement in plants. *New Phytol.* **197**, 1095-1103 (2013).
- 481 16. Rieseberg, L. H. & Wendel, J. F. Introgression and its consequences in plants. *Hybrid Zones and*
482 *the Evolutionary Process* **70**, 70-109 (1993).
- 483 17. Taylor, S. A. & Larson, E. L. Insights from genomes into the evolutionary importance and
484 prevalence of hybridization in nature. *Nature Ecology & Evolution* **3**, 170-177 (2019).

- 485 18. Whitney, K. D., Randell, R. A. & Rieseberg, L. H. Adaptive introgression of abiotic tolerance
486 traits in the sunflower *Helianthus annuus*. *New Phytol.* **187**, 230-239 (2010).
- 487 19. Suarez-Gonzalez, A., Lexer, C. & Cronk, Q. C. B. Adaptive introgression: a plant perspective.
488 *Biol. Lett.* **14**, 10.1098/rsbl.2017.0688 (2018).
- 489 20. Marques, D. A., Meier, J. I. & Seehausen, O. A combinatorial view on speciation and adaptive
490 radiation. *Trends in Ecology & Evolution* **34**, 531-544 (2019).
- 491 21. Lamichhaney, S. *et al.* Rapid hybrid speciation in Darwin's finches. *Science* **359**, 224-228 (2018).
- 492 22. Rieseberg, L. H. *et al.* Major ecological transitions in wild sunflowers facilitated by hybridization.
493 *Science* **301**, 1211-1216 (2003).
- 494 23. Meier, J. I. *et al.* Ancient hybridization fuels rapid cichlid fish adaptive radiations. *Nature*
495 *Communications* **8**, 14363 (2017).
- 496 24. Payseur, B. A. Using differential introgression in hybrid zones to identify genomic regions
497 involved in speciation. *Molecular Ecology Resources* **10**, 806-820 (2010).
- 498 25. Gompert, Z., Parchman, T. L. & Buerkle, C. A. Genomics of isolation in hybrids. *Philos. Trans.*
499 *R. Soc. Lond. B. Biol. Sci.* **367**, 439-450 (2012).
- 500 26. Hamilton, J. A. & Aitken, S. N. Genetic and morphological structure of a spruce hybrid (*Picea*
501 *sitchensis* × *P. glauca*) zone along a climatic gradient. *Am. J. Bot.* **100**, 1651-1662 (2013).
- 502 27. Sullivan, A. R., Owusu, S. A., Weber, J. A., Hipp, A. L. & Gailing, O. Hybridization and
503 divergence in multi-species oak (*Quercus*) communities. *Bot. J. Linn. Soc.* **181**, 99-114 (2016).
- 504 28. Abbott, R. J. *et al.* Hybridization and speciation. *J. Evol. Biol.* **26**, 229-246 (2013).
- 505 29. Seehausen, O. *et al.* Genomics and the origin of species. *Nature Reviews Genetics* **15**, 176-192
506 (2014).
- 507 30. Schley, R. J. *et al.* Is Amazonia a 'museum' for Neotropical trees? The evolution of the Brownea
508 clade (Detarioideae, Leguminosae). *Mol. Phylogenet. Evol.* **126**, 279-292 (2018).
- 509 31. Crawford, T. & Nelson, E. Irish Horticulturists. I: WH Crawford. *Garden History* **7**, 23-26 (1979).
- 510 32. Backer, C. A. in *Schoolflora voor Java* 418 (Visser & Co., Weltevreden, Java, Dutch East Indies,
511 1911).
- 512 33. Pérez, Á J., Klitgård, B. B., Saslis-Lagoudakis, C. & Valencia, R. *Brownea jaramilloi*
513 (Leguminosae: Caesalpinioideae), a new, over-looked species endemic to the Ecuadorian Amazon .
514 *Kew Bull.* **68**, 157-162 (2013).
- 515 34. Klitgaard, B. B. Ecuadorian *Brownea* and *Browneopsis* (Leguminosae-Caesalpinioideae):
516 taxonomy, palynology, and morphology. *Nord. J. Bot.* **11**, 433-449 (1991).
- 517 35. ter Steege, H. *et al.* Hyperdominance in the Amazonian tree flora. *Science* **342**, 1243092 (2013).
- 518 36. Zhang, C., Rabiee, M., Sayyari, E. & Mirarab, S. ASTRAL-III: polynomial time species tree
519 reconstruction from partially resolved gene trees. *BMC Bioinformatics* **19**, 153 (2018).

- 520 37. Stamatakis, A. RAxML version 8: a tool for phylogenetic analysis and post-analysis of large
521 phylogenies. *Bioinformatics* **30**, 1312-1313 (2014).
- 522 38. Huson, D. H. & Bryant, D. Application of phylogenetic networks in evolutionary studies. *Mol.*
523 *Biol. Evol.* **23**, 254-267 (2005).
- 524 39. Raj, A., Stephens, M. & Pritchard, J. K. fastSTRUCTURE: variational inference of population
525 structure in large SNP data sets. *Genetics* **197**, 573-589 (2014).
- 526 40. Anderson, E. C. & Thompson, E. A. A model-based method for identifying species hybrids using
527 multilocus genetic data. *Genetics* **160**, 1217-1229 (2002).
- 528 41. Burbrink, F. T. & Gehara, M. The biogeography of deep time phylogenetic reticulation. *Syst. Biol.*
529 **67**, 743-744 (2018).
- 530 42. Pennington, R. T. & Lavin, M. The contrasting nature of woody plant species in different
531 neotropical forest biomes reflects differences in ecological stability. *New Phytol.* **210**, 25-37 (2016).
- 532 43. Lepais, O. & Gerber, S. Reproductive patterns shape introgression dynamics and species
533 succession within the European white oak species complex. *Evolution* **65**, 156-170 (2011).
- 534 44. Morales-Briones, D. F., Liston, A. & Tank, D. C. Phylogenomic analyses reveal a deep history of
535 hybridization and polyploidy in the Neotropical genus *Lachemilla* (Rosaceae). *New Phytol.* **218**,
536 1668-1684 (2018).
- 537 45. Sweigart, A. L. & Willis, J. H. Patterns of nucleotide diversity in two species of *Mimulus* are
538 affected by mating system and asymmetric introgression. *Evolution* **57**, 2490-2506 (2003).
- 539 46. Buggs, R. J. & Pannell, J. R. Rapid displacement of a monoecious plant lineage is due to pollen
540 swamping by a dioecious relative. *Current Biology* **16**, 996-1000 (2006).
- 541 47. Petit, R. J., Bodénès, C., Ducouso, A., Roussel, G. & Kremer, A. Hybridization as a mechanism
542 of invasion in oaks. *New Phytol.* **161**, 151-164 (2004).
- 543 48. Balao, F., Casimiro-Soriguer, R., García-Castaño, J. L., Terrab, A. & Talavera, S. Big thistle eats
544 the little thistle: does unidirectional introgressive hybridization endanger the conservation of
545 *Onopordum hinojense*? *New Phytol.* **206**, 448-458 (2015).
- 546 49. Yang, W. *et al.* Genomic evidence for asymmetric introgression by sexual selection in the
547 common wall lizard. *Mol. Ecol.* **27**, 4213-4224 (2018).
- 548 50. Scascitelli, M. *et al.* Genome scan of hybridizing sunflowers from Texas (*Helianthus annuus* and
549 *H. debilis*) reveals asymmetric patterns of introgression and small islands of genomic differentiation.
550 *Mol. Ecol.* **19**, 521-541 (2010).
- 551 51. Arnold, M. L., Tang, S., Knapp, S. J. & Martin, N. H. Asymmetric introgressive hybridization
552 among Louisiana Iris species. *Genes* **1**, 9-22 (2010).
- 553 52. Mallet, J. Hybridization as an invasion of the genome. *Trends in Ecology & Evolution* **20**, 229-237
554 (2005).

- 555 53. Kenzo, T. *et al.* Overlapping flowering periods among *Shorea* species and high growth
556 performance of hybrid seedlings promote hybridization and introgression in a tropical rainforest of
557 Singapore. *For. Ecol. Manage.* **435**, 38-44 (2019).
- 558 54. Kamiya, K. *et al.* Morphological and molecular evidence of natural hybridization in *Shorea*
559 (Dipterocarpaceae). *Tree Genetics & Genomes* **7**, 297-306 (2011).
- 560 55. Lo, E. Testing hybridization hypotheses and evaluating the evolutionary potential of hybrids in
561 mangrove plant species. *J. Evol. Biol.* **23**, 2249-2261 (2010).
- 562 56. Solís-Lemus, C., Bastide, P. & Ané, C. PhyloNetworks: a package for phylogenetic networks.
563 *Mol. Biol. Evol.* **34**, 3292-3298 (2017).
- 564 57. Legume Phylogeny Working Group. A new subfamily classification of the Leguminosae based on
565 a taxonomically comprehensive phylogeny: The Legume Phylogeny Working Group (LPWG). *Taxon*
566 **66**, 44-77 (2017).
- 567 58. Andrews, S. FastQC: a quality control tool for high throughput sequence data. Available online
568 at <http://www.bioinformatics.babraham.ac.uk/projects/fastqc>. (2010).
- 569 59. Bolger, A. M., Lohse, M. & Usadel, B. Trimmomatic: a flexible trimmer for Illumina sequence
570 data. *Bioinformatics* **30**, 2114-2120 (2014).
- 571 60. Johnson, M. G. *et al.* HybPiper: Extracting coding sequence and introns for phylogenetics from
572 high-throughput sequencing reads using target enrichment. *App. Plant. Sci.* **4**, 1600016 (2016).
- 573 61. Python Software Foundation. Python Language Reference, version 2.7. <http://www.python.org>
574 (2010).
- 575 62. Katoh, K. & Standley, D. M. MAFFT multiple sequence alignment software version 7:
576 improvements in performance and usability. *Mol. Biol. Evol.* **30**, 772-780 (2013).
- 577 63. Smith, S. A., Moore, M. J., Brown, J. W. & Yang, Y. Analysis of phylogenomic datasets reveals
578 conflict, concordance, and gene duplications with examples from animals and plants. *BMC*
579 *Evolutionary Biology* **15**, Published online: DOI 10.1186/s12862-015-0423-0 (2015).
- 580 64. Bezanson, J., Edelman, A., Karpinski, S. & Shah, V. B. Julia: A fresh approach to numerical
581 computing. *SIAM Rev* **59**, 65-98 (2017).
- 582 65. Stenz, N. W., Larget, B., Baum, D. A. & Ané, C. Exploring tree-like and non-tree-like patterns
583 using genome sequences: an example using the inbreeding plant species *Arabidopsis thaliana* (L.)
584 Heynh. *Syst. Biol.* **64**, 809-823 (2015).
- 585 66. R Development Core Team. R: A language and environment for statistical computing. Available
586 at: <http://www.R-project.org/>. (2013).
- 587 67. Ho, L. S. T. & Ané, C. A linear-time algorithm for Gaussian and non-Gaussian trait evolution
588 models. *Syst. Biol.* **63**, 397-408 (2014).
- 589 68. Peterson, B. K., Weber, J. N., Kay, E. H., Fisher, H. S. & Hoekstra, H. E. Double digest RADseq:
590 an inexpensive method for de novo SNP discovery and genotyping in model and non-model species.
591 *PloS one* **7**, e37135 (2012).

- 592 69. Catchen, J. M., Amores, A., Hohenlohe, P., Cresko, W. & Postlethwait, J. H. Stacks: building and
593 genotyping Loci de novo from short-read sequences. *G3 (Bethesda)* **1**, 171-182 (2011).
- 594 70. Wickham, H. in *ggplot2: elegant graphics for data analysis* (Springer, 2016).
- 595 71. Gompert, Z. & Buerkle, C. A. Bayesian estimation of genomic clines. *Mol. Ecol.* **20**, 2111-2127
596 (2011).
- 597 72. Rambaut, A., Suchard, M. A., Xie, D. & Drummond, A. J. Tracer.
598 <http://tree.bio.ed.ac.uk/software/tracer/> **1.6** (2015).
- 599 73. Plummer, M., Best, N., Cowles, K. & Vines, K. CODA: convergence diagnosis and output
600 analysis for MCMC. *R news* **6**, 7-11 (2006).
- 601 74. Geweke, J. in *Evaluating the accuracy of sampling-based approaches to the calculation of*
602 *posterior moments* (Federal Reserve Bank of Minneapolis, Research Department, Minneapolis, MN,
603 USA, 1991).

604

605 Acknowledgements

606 Laboratory work, fieldwork and herbarium visits to NY and US were funded by the NERC SSCP
607 DTP, and a Genetics society Heredity Fieldwork grant funded part of the fieldwork in Ecuador.
608 Phylogenomic sequencing was also part-funded by a grant from the Royal Botanic Gardens, Kew.
609 Thank you to Dario Ojeda for baits and associated help, to Laszlo Csiba, Penny Malakasi, Niroshini
610 Epitawalage, Dion Devey, Robyn Cowan and Steven Dodsworth for help in the laboratory, and to
611 Gregor Gilfillan at the Norwegian sequencing centre for help with ddRAD sequencing. Thank you to
612 Andres Melo Burbano for his help during fieldwork, as well as to Renato Valencia and Álvaro Pérez
613 for helping to coordinate fieldwork in Ecuador. Thanks to Colin Hughes, Jeff Doyle and Matteo
614 Fumagalli for comments on analytical methods, and to Peter Raven and Benjamin Torke for their
615 comments on the rarity of hybridization in tropical trees.

616

617 Collection, transport and extraction of genetic material from plant accessions collected in Yasuní
618 National Park were authorised by Ecuador's Environment Ministry. Permits were issued with the
619 following authorization numbers:

- 620 • **Collection permit:** 021-2016-IC-FAU-FLO-DPAO-PNY;
- 621 • **Mobilization permit:** 037-2016-MOV-FLO-MAE-DPAO;

- 622 • **Export permit:** 208-2019-EXP-CM-FAU-DNB/MA; and
623 • **Genetic research permit (Contrato Marco):** MAE-DNB-CM-2018-0082

624

625 Author Contributions

626 R.J.S. conceived this study and performed all analyses, supervised by T.B., F.F. and B.K. Population
627 genomic data were generated by R.J.S., and phylogenomic data were generated by R.J.S., I.K. and I.L.
628 Baits for hybrid capture were provided by M.d.l.E. R.J.S. wrote the first draft of the manuscript with
629 contributions from R.T.P., O.A.P.E., A.J.H., M.d.l.E., I.L., T.B., F.F. and B.K.

630

631 Competing Interests

632 The authors declare no competing financial interest.

633

634 Figure Legends

635 **Figure 1:** Two co-occurring *Brownea* lineages (*Brownea grandiceps* (photograph © Rowan Schley)
636 and *Brownea jaramilloi* (photograph © Xavier Cornejo)) as well as their putative hybrid *Brownea*
637 “rosada” (photograph © J. L. Clark).

638

639 **Figure 2:** *ASTRAL* species tree inferred from *RAxML* gene trees using the multi-species coalescent
640 model. Numbers at nodes of the tree signify local posterior probability (LPP) values, a measure of
641 support for each quadripartition. Taxa within the red box belong to the ‘Grandiceps’ subclade, taxa
642 within the green box belong to the ‘Coccinea’ subclade, taxa within the pink box represent the
643 ‘Stenantha’ subclade and those within the blue box belong to the ‘Chocóan’ subclade. Images show
644 inflorescences of species within *Brownea*- species shown are, from top to bottom: *B. grandiceps*
645 (photograph © Rowan Schley), *B. jaramilloi* (photograph © Xavier Cornejo), *B. macrophylla*

646 (photograph © Bente Klitgaard), *B. coccinea* subsp. *capitella* (photograph © Xavier Cornejo), *B.*
647 *longipedicellata* (photograph © Domingos Cardoso) and *B. multijuga* (photograph © Bente
648 Klitgaard).

649

650 **Figure 3:** Phylogenetic network with one hybridization event ($h = 2$), estimated using *SNaQ!* in the
651 Julia package *PhyloNetworks*. Light blue horizontal branches indicate inferred hybridization events,
652 and numbers next to the branches show the estimated proportion of genes contributed by each lineage
653 in the hybridization event. Red branches signify the ancestral lineage and what proportion of the
654 modern lineage's genes were contributed from it. Taxa were chosen in order to represent one
655 accession per lineage, as per the assumptions of *PhyloNetworks*, and the individual with the highest
656 gene recovery was used for each lineage. Coloured boxes containing taxa are described in the legend
657 of Fig. 2.

658

659 **Figure 4:** Principal component analysis of genotype data for all SNPs inferred at all loci. Individuals
660 are coded by colour and point shape: red circles denote individuals identified as *B. grandiceps*, yellow
661 circles denote individuals identified as *B. jaramilloi*, and blue triangles denote putative hybrid
662 individuals (*B.* “rosada”). The amount of the genetic variation explained by each principle component
663 is shown next to axes, which are labelled PC1 and PC2.

664

665 **Figure 5:** *fastSTRUCTURE* plot, indicating ancestry proportions for two populations ($K = 2$). The
666 ‘populations’ correspond to two different species: *B. grandiceps* (shown in red) and *B. jaramilloi*
667 (shown in yellow). Each individual accession is represented by a column, and the proportion of
668 ancestry from either species (mean Q) is proportional to the length of different coloured bars in each
669 column. Individuals identified as *B.* “rosada” are marked with a blue box and a blue triangle beneath
670 their column. All taxa to the left and right of these boxes were identified as *B. jaramilloi* and *B.*
671 *grandiceps*, respectively.